This pdf file consists of figures containing photographs, and their captions, scanned from:

FAULT-RELATED OCEANIC AND EMPLACEMENT-AGE SERPENTINIZATION IN THE JOSEPHINE OPHIOLITE OF NW CALIFORNIA AND SW OREGON

by

Angela J. Coulton, B.A.

A Dissertation
Submitted to the State University of New York at Albany
in Partial Fulfillment
of the Requirements for the Degree of
Doctor of Philosophy

College of Arts and Sciences
Department of Geological Sciences
1995

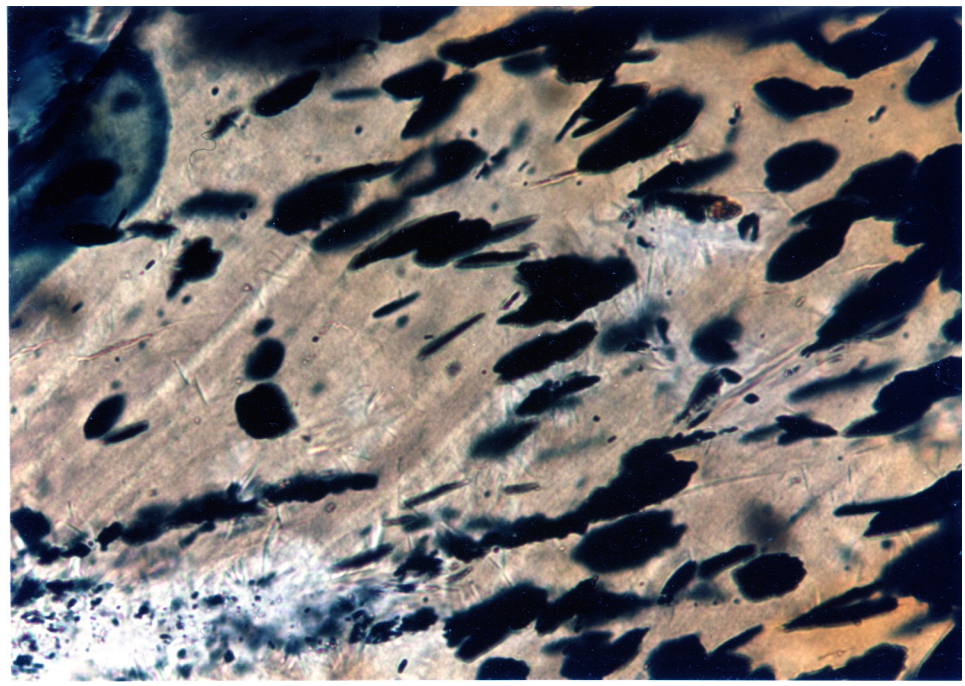

Figure 3-4 Fe-Ni sulfides (opaque ellipsoids), identified by electron microprobe, within lizardite (yellow/brown). Field of view approximately 0.5 mm, plane polarized light.

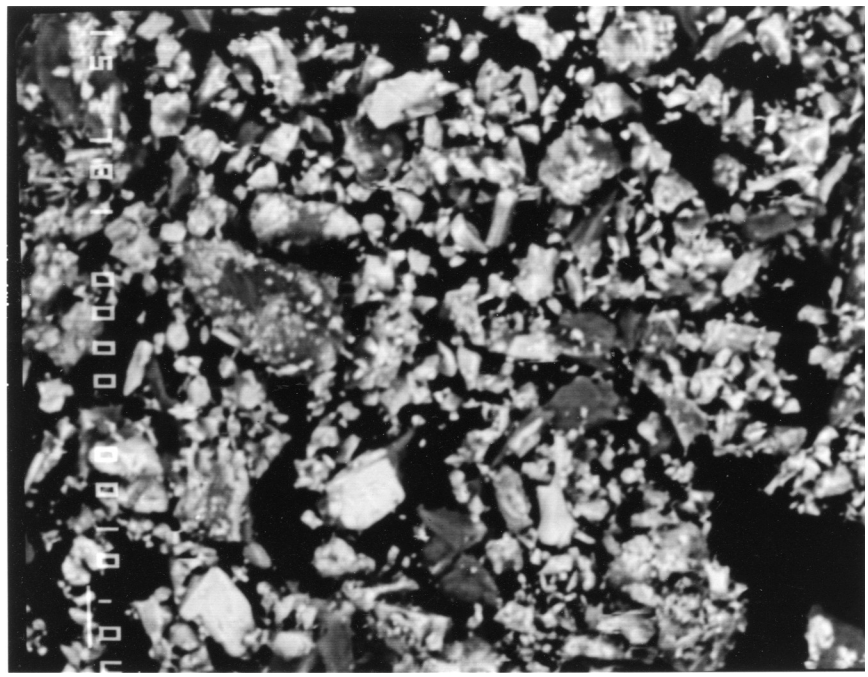

Figure 3-5 Back-scattered electron image of magnetite powder. Light grey/white grains are magnetite, dark grains are serpentine.

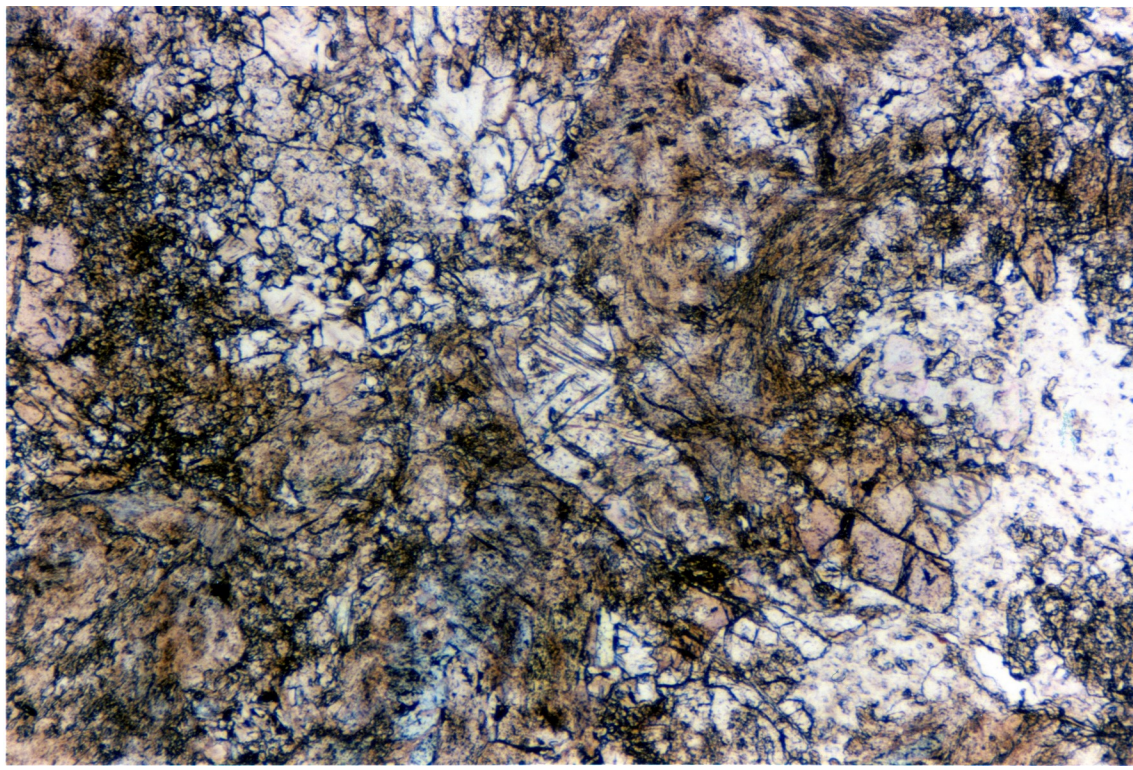

Figure 4-1 Photomicrograph of rodingitized gabbro from PCSZ (Sample PC7a). Rodingite minerals identified in thin-section include hydrogarnet (cluster of colorless, high relief, rounded crystals in upper left) and zoisite (large, tabular, pale brown crystals in lower right). Field of view 2 mm, PPL.

Figure 4-2 Hand specimens of hornblende andesite (left, sample IL5) and Fe-Ti enriched diabase (right, sample IL6) from dikes intruding serpentinites at junction of Josephine Creek and Illinois River. Coin diameter 2.5 cm.

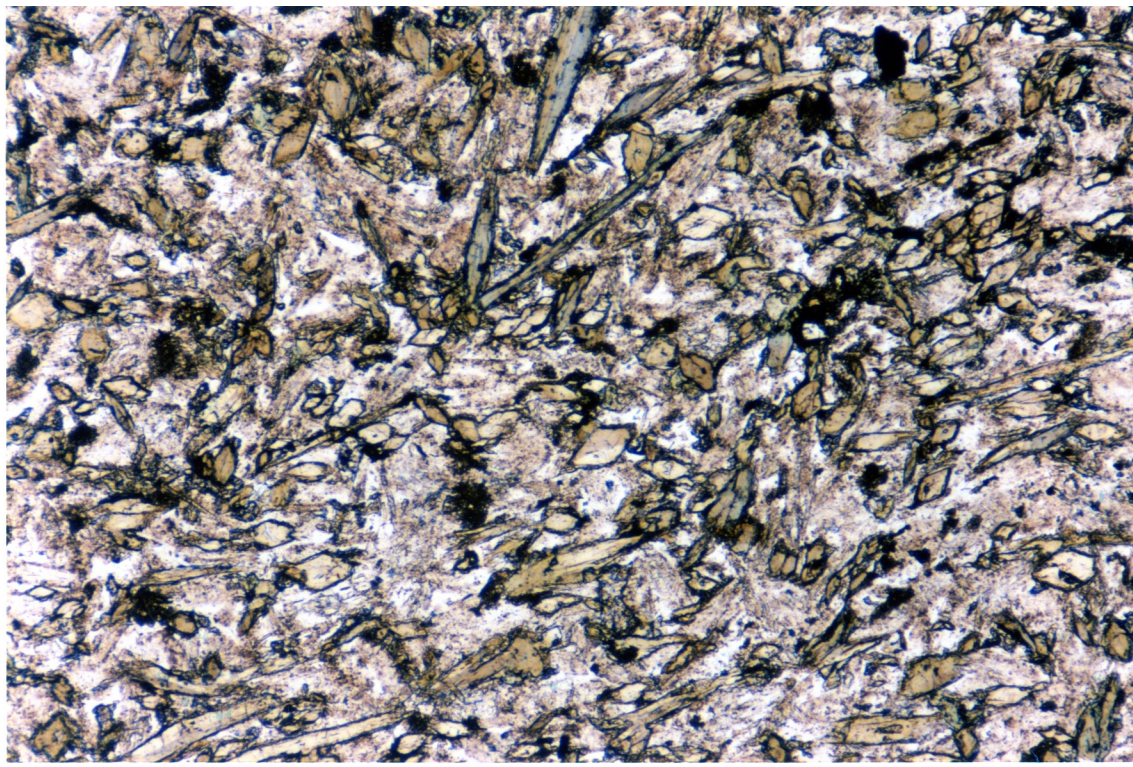

Figure 4-3 Photomicrograph of hornblende andesite dike containing abundant igneous hornblende in a groundmass of sausseritized plagioclase. Field of view 2 mm, PPL.

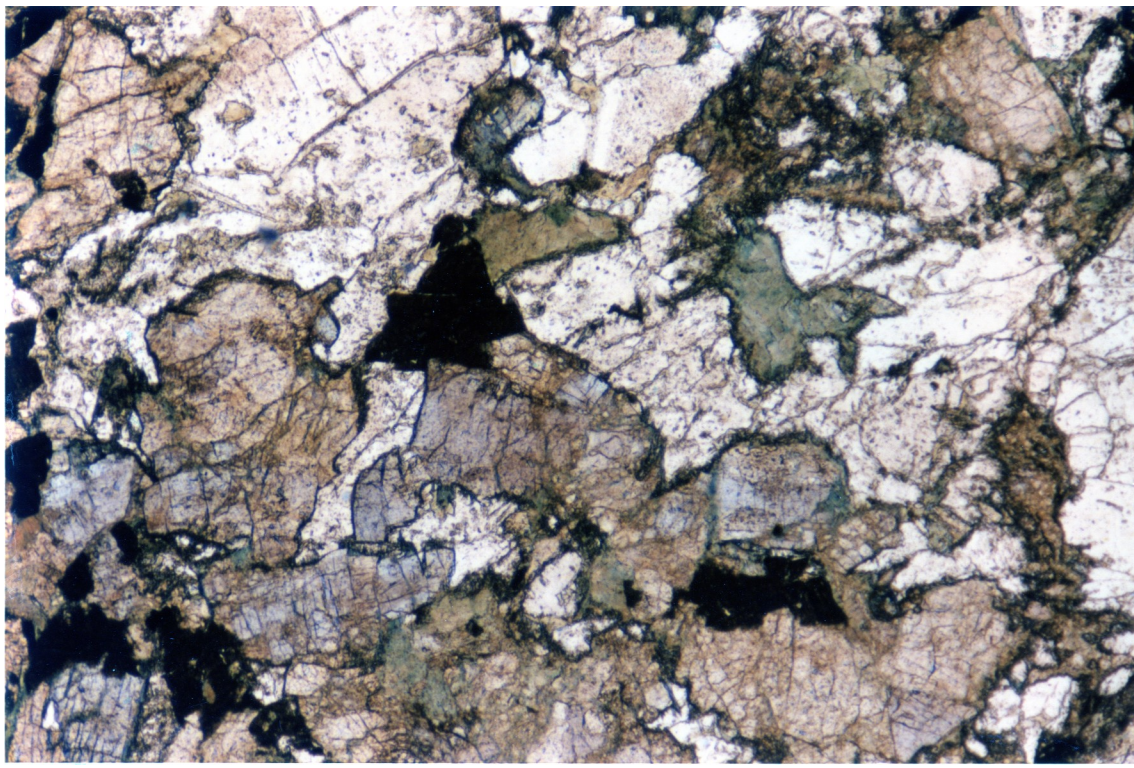

Figure 4-4 Photomicrograph of Fe-Ti enriched microgabbro from the JCSZ (sample JC23) Pale pink-brown mineral is titanaugite, colorless mineral is plagioclase, almost opaque mineral is titanite. Minor secondary alteration indicated by patches of chlorite. Field of view 4 mm, PPL.

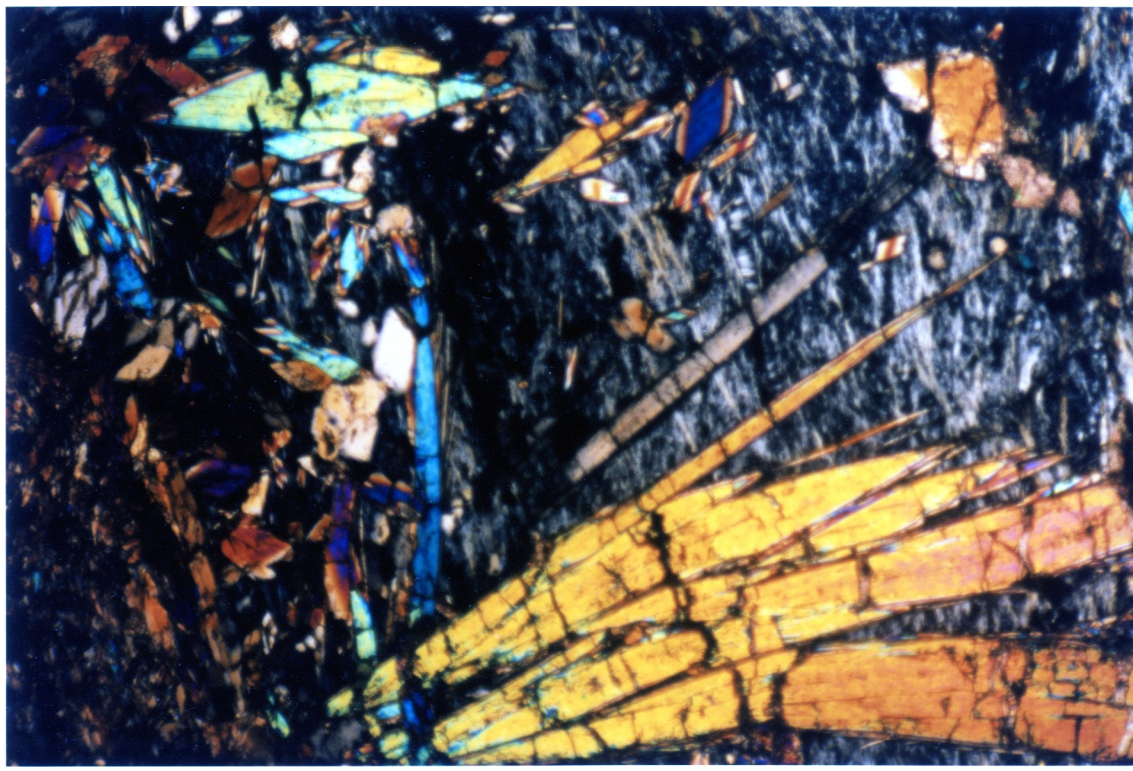

Figure 4-5 Contact aureole in foliated antigorite serpentinite adjacent to deformed amphibolite dike in TRSZ (Sample GT17b). Coarse-grained tremolite cuts across antigorite (gray) with strong preferred orientation, indicating crystallization within aureole continued after ductile deformation of serpentinite. Field of view 2 mm, XPL.

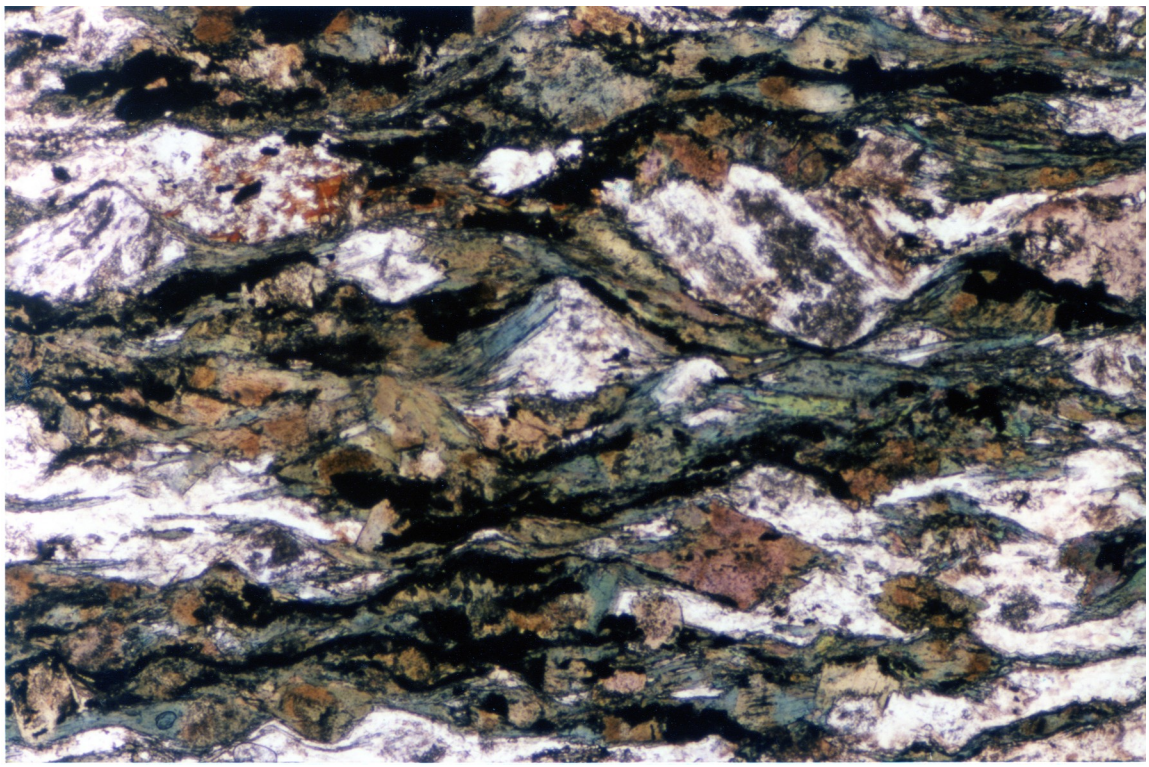

Figure 4-6 Ductilely deformed amphibolite dike from the TRSZ (Sample GT17c). Foliation defined by green/brown hornblende and opaque minerals. Sausseritized plagioclase and hornblende occur as porphyroclasts. Field of view 4 mm, PPL.

A

B

Figure 4-7 Dikes cross-cutting blocky sheared serpentinites in JCSZ. (A) Hornblende andesite dike cuts across steeply dipping, N-S trending foliation defined by block margins (B) 10 cm wide dike curves around block margins. Note narrow contact aureole in serpentinite along dike margin.

A

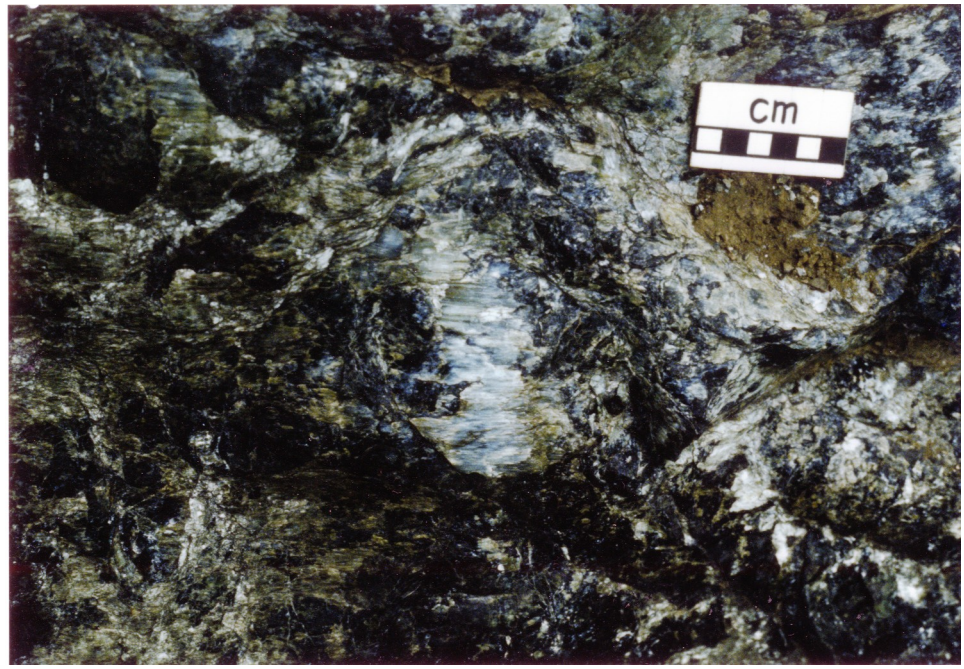

B

Figure 4-8 Serpentine slickenfibers along margins of serpentinized blocks (A) Stepped serpentine slickenfibers along block margin in PCSZ. (B) Serpentine + magnetite slickenfibers within JCSZ.

Figure 4-9 Hornblende-bearing dikes cross-cutting Fe-Ti microgabbro, within JCSZ, 20 m north of junction of Canyon Creek with Josephine Creek.

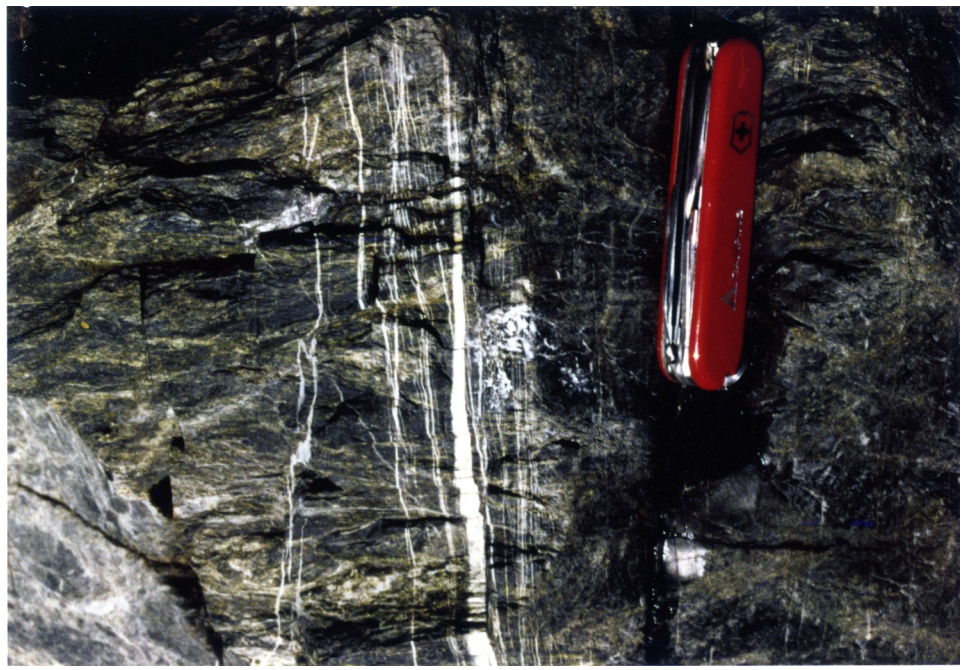

Figure 4-10 Serpentine + dolomite fibrous extension veins cross-cutting strongly foliated serpentinite within PCSZ (sample PCM 23)

Figure 4-11 Hornblende andesite dike intruding foliated serpentinite in PCSZ (adjacent to area of Figure 4-10). Extension veins of similar orientation cross-cut both serpentinite and dike, indicating fibrous veins post-date emplacement-age dike intrusion. Scale bar on dike is 5 cm.

A

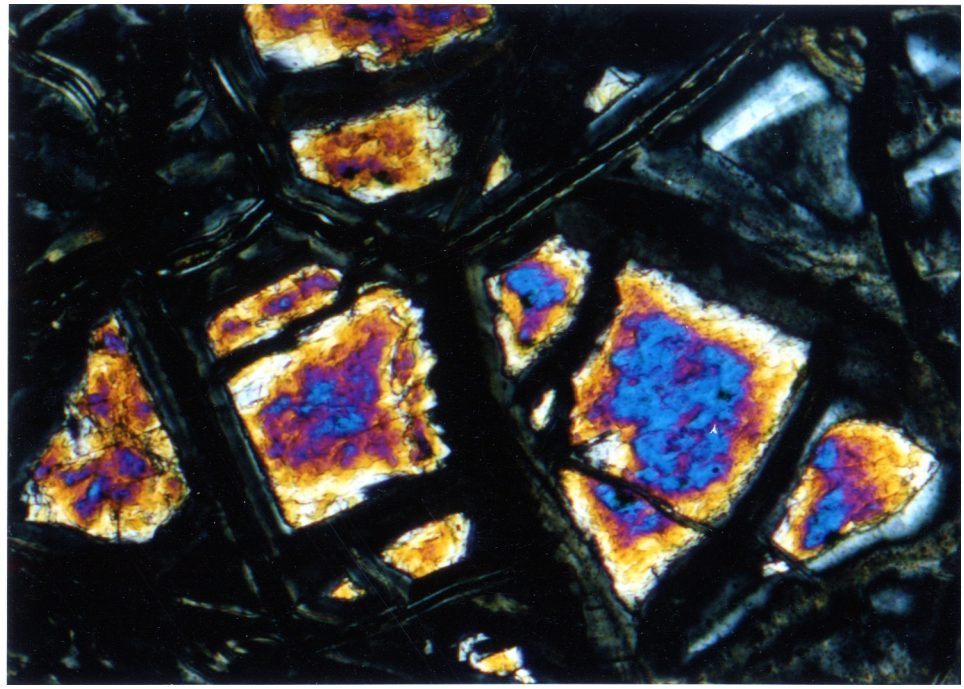

B

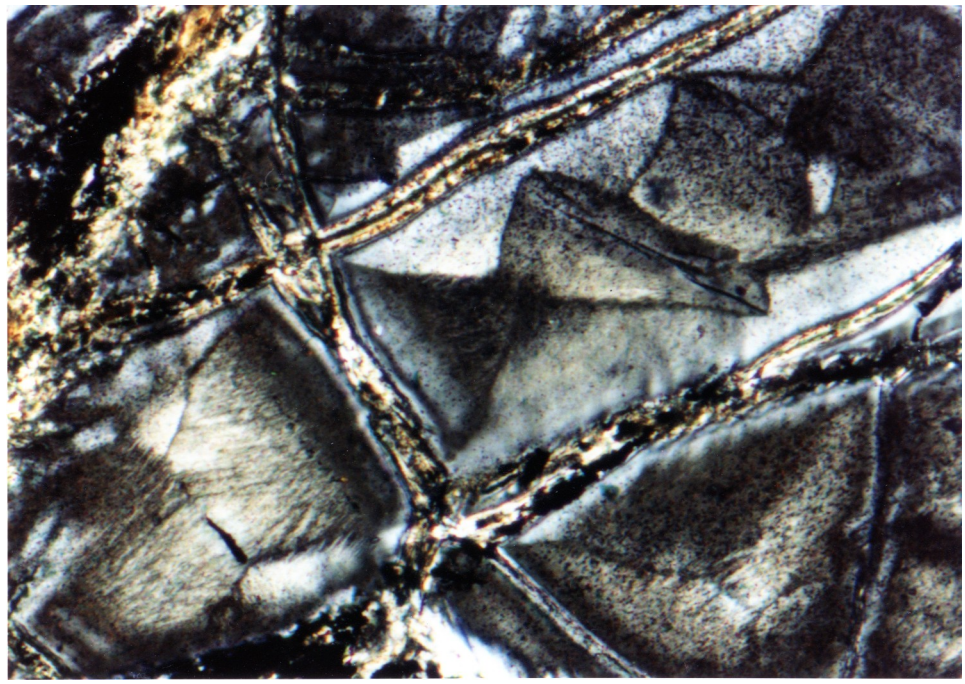

Figure 4-12 (A) Partial serpentinization. Mesh texture serpentinite with lizardite mesh rims an olivine mesh centers. (Sample RC8) Field of view 1 mm (B) Complete serpentinization. Mesh/hourglass texture. Lizardite + magnetite mesh rims, hourglass structure lizardite in mesh center. (Sample RC9) Field of view 1 mm. Both XPL. Samples from shear zone at base of peridotite west of Low Divide shear zone.

A

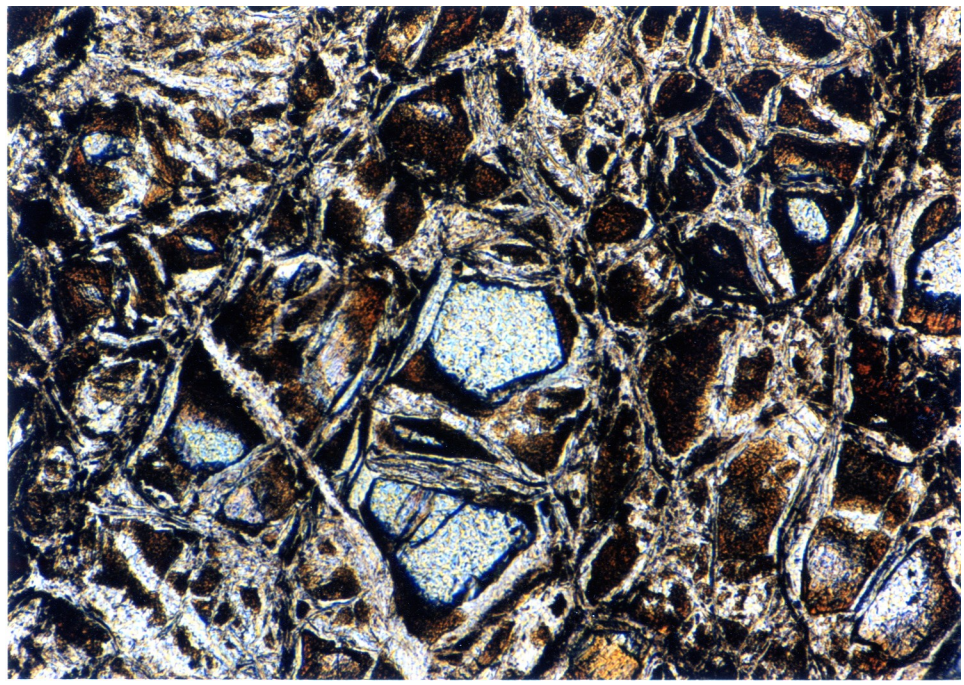

B

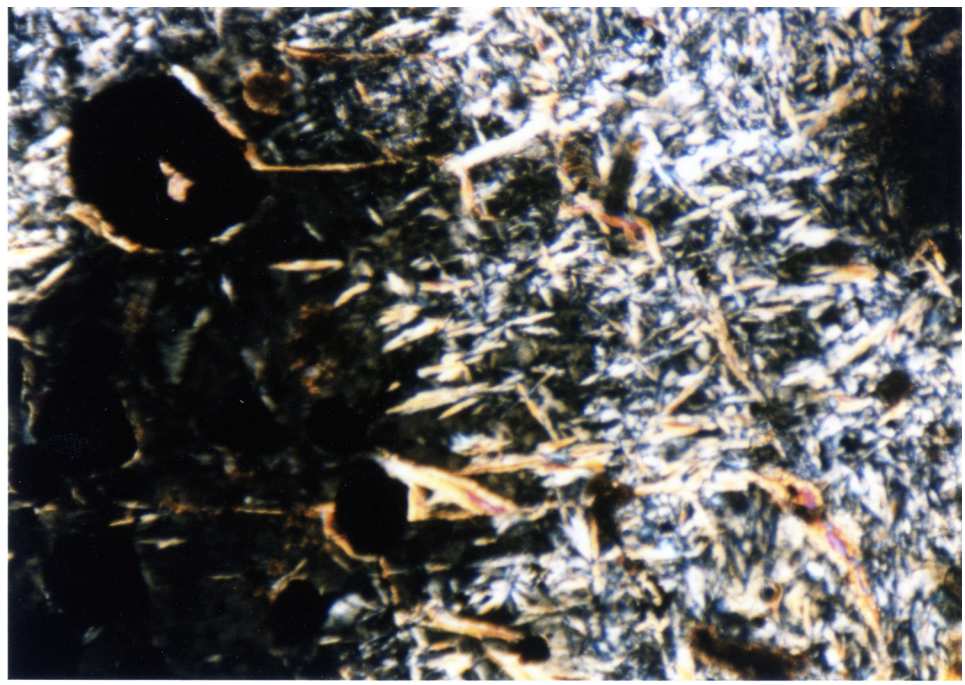

Figure 4-13 (A) Partially serpentinized dunite exhibiting mesh texture. Brucite (red-brown) occurs between mesh rims and centers (sample LD60, LDSZ) Field of view 2 mm, PPL. (B) Partially recrystallized, lizardite + antigorite serpentinite. Antigorite has a non-pseudomorphic, interpenetrating texture (sample PCM5, PCSZ). Field of view 2 mm, XPL.

A

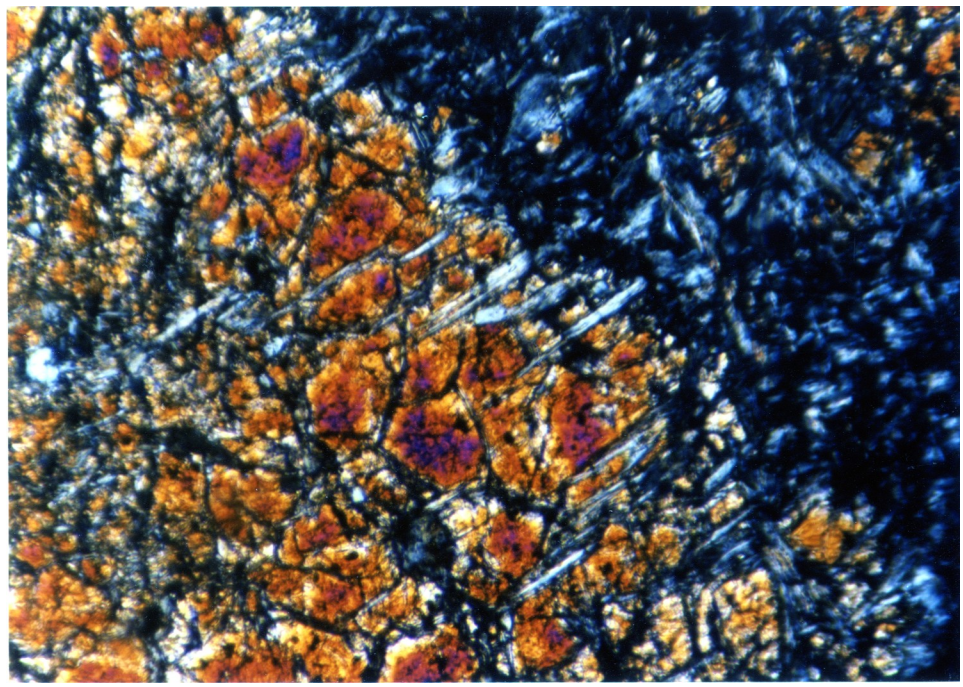

B

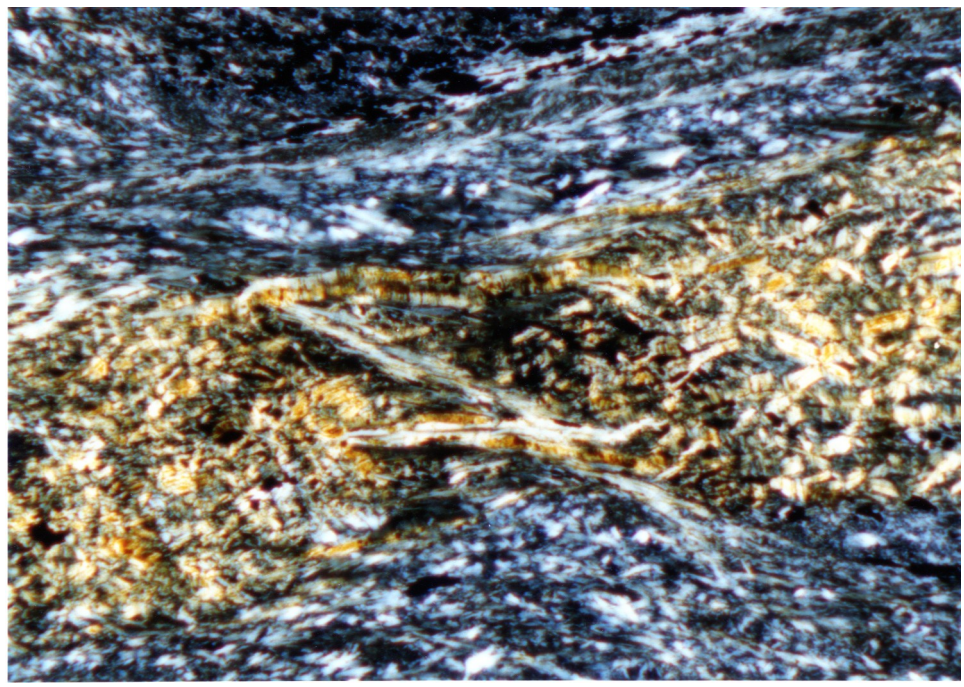

Figure 4-14 (A) Partially serpentinized olivine with antigorite blades nucleating along olivine/ serpentine boundary (sample GT14, TRSZ). Field of view 1.5 mm. (B) Antigorite shear band, cross-cutting lizardite band within serpentine mylonite (sample GT4c, TRSZ). Field of view 3 mm. Both XPL.

A

B

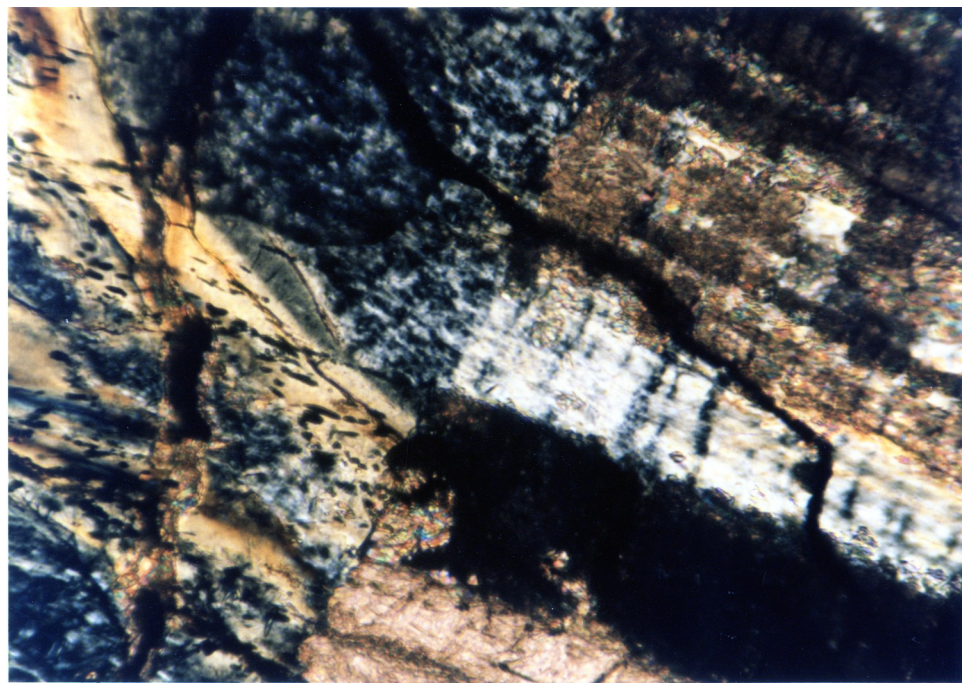

Figure 4-15 (A) Lizardite + magnetite vein cross cutting mesh texture lizardite + brucite serpentinite (sample LD2, LDSZ). Note recrystallization along vein margin. Late transverse veins may be chrysotile. Field of view 4 mm (B) Antigorite + dolomite extension vein (lower left) cross-cutting antigorite + lizardite serpentinite. Lizardite yellow, antigorite first-order grey/white. Dolomite shows high relief and extreme birefringence. Field of view 1 mm. Both XPL.

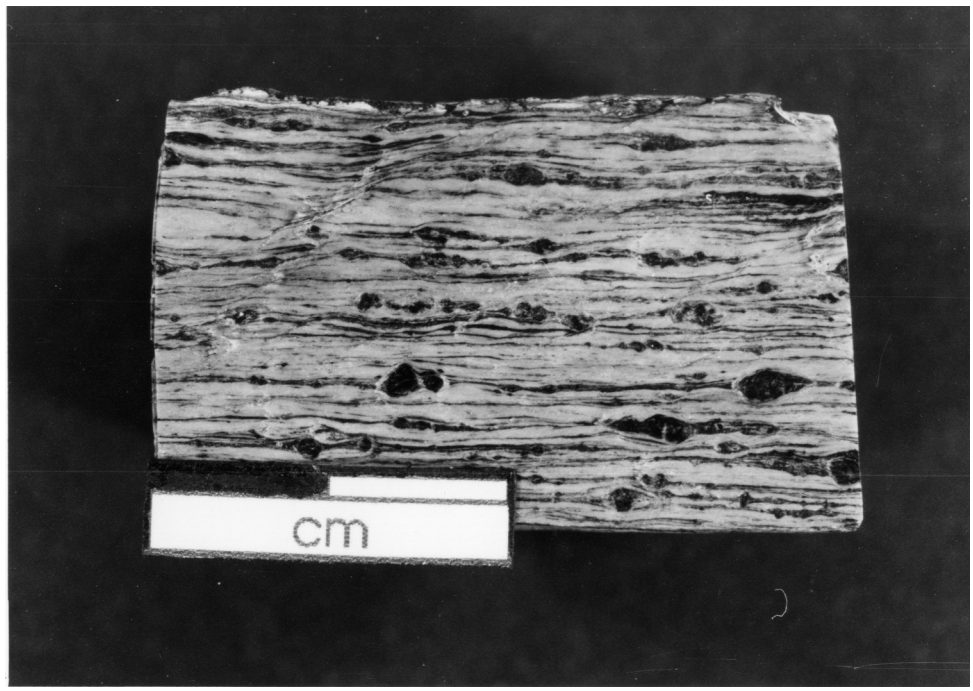

Figure 5-2 Foliation, rotated magnetite porphyroclasts, and shear bands in hand specimen of serpentinite mylonite. Sample KG-752b, Red Mountain shear zone (Norrell and others, 1989). Dextral shear band in upper left corner of sample.

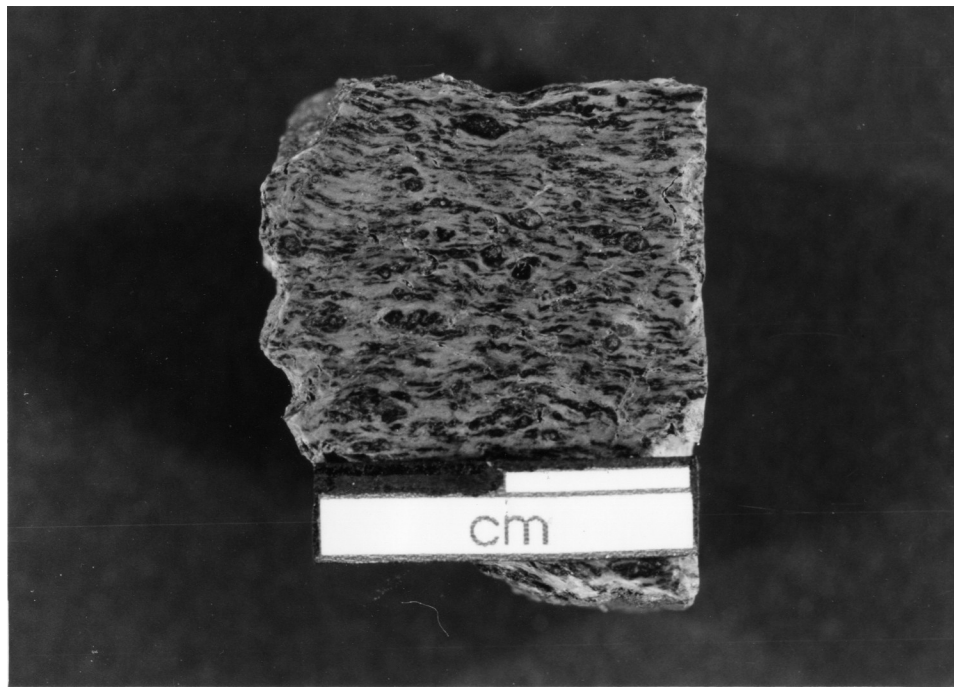

Figure 5-3 Serpentinite mylonite of figure 5.2, cut face perpendicular to foliation and lineation.

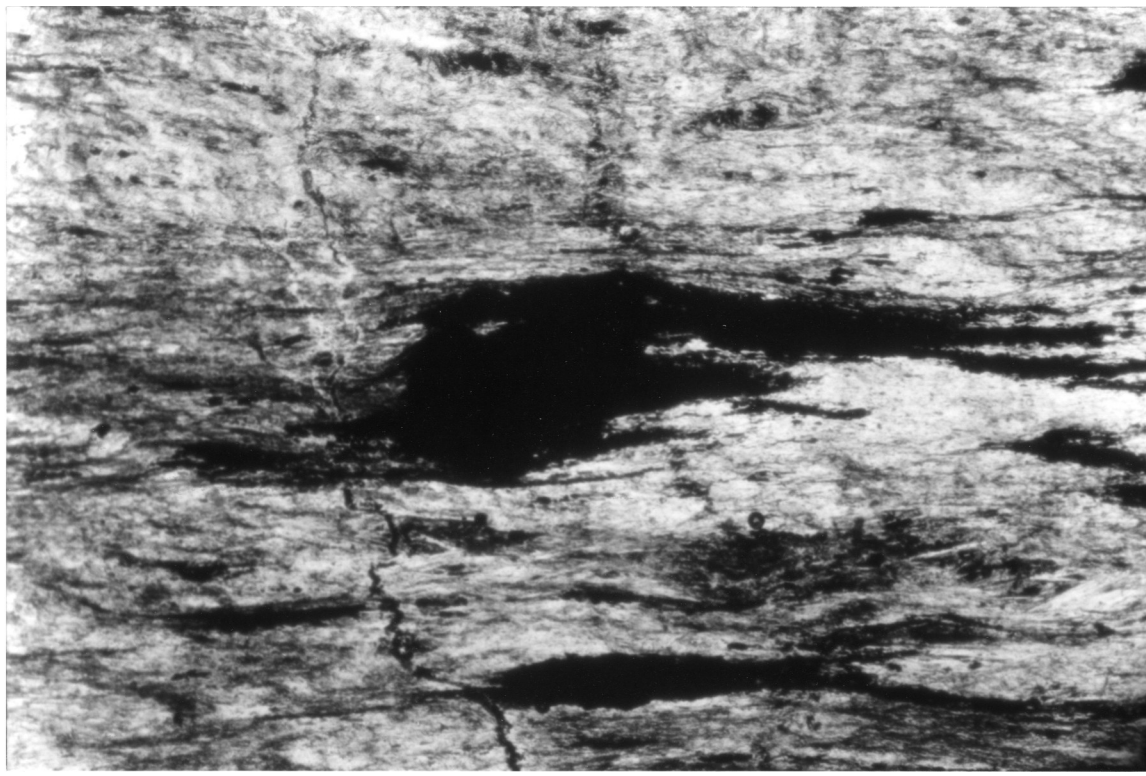

Figure 5-4 Asymmetric magnetite porphyroclast within fine-grained antigorite mylonite matrix. Sample GT7c, Toll Road Shear Zone (Norrell and others, 1989). Field of view 3 mm.

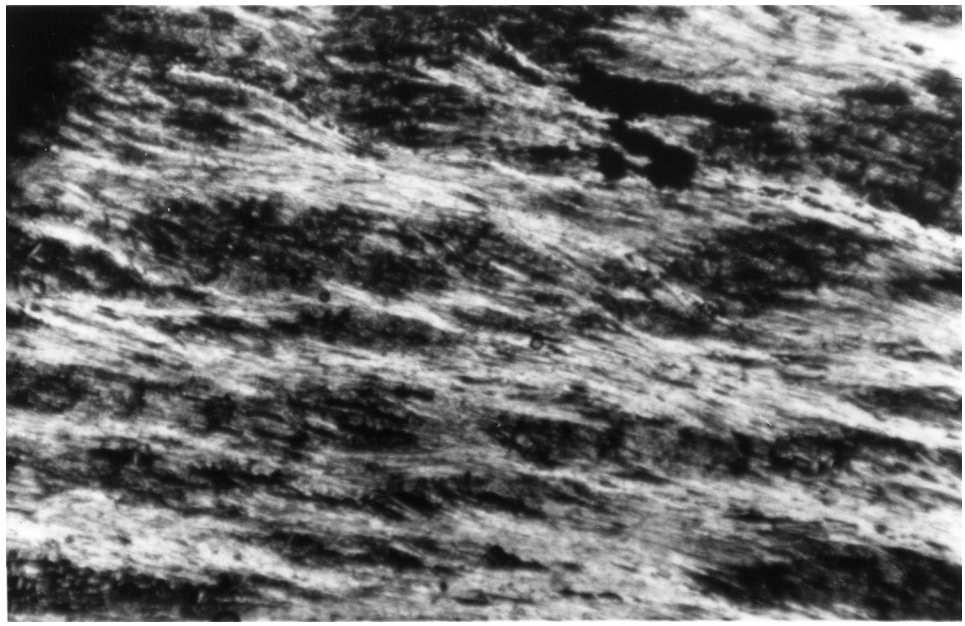

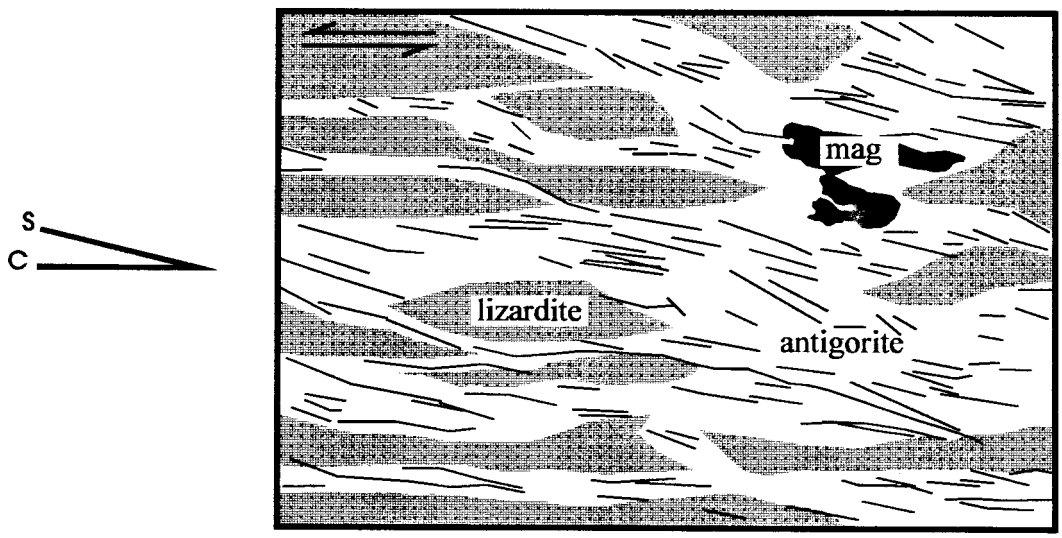

Figure 5-5 S-C fabric in antigorite mylonite, Toll Road Shear Zone (Norrell and others, 1989). Field of view 4mm.

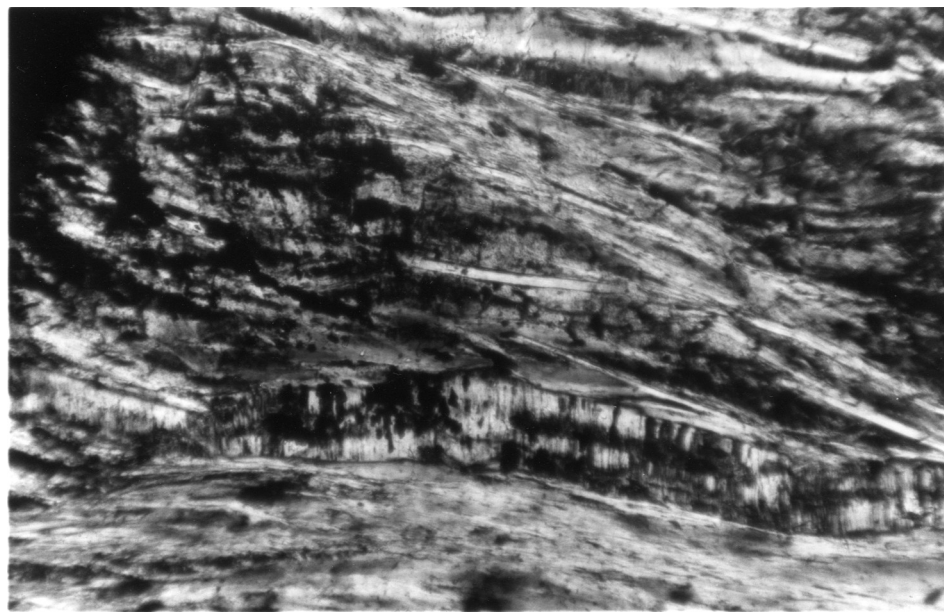

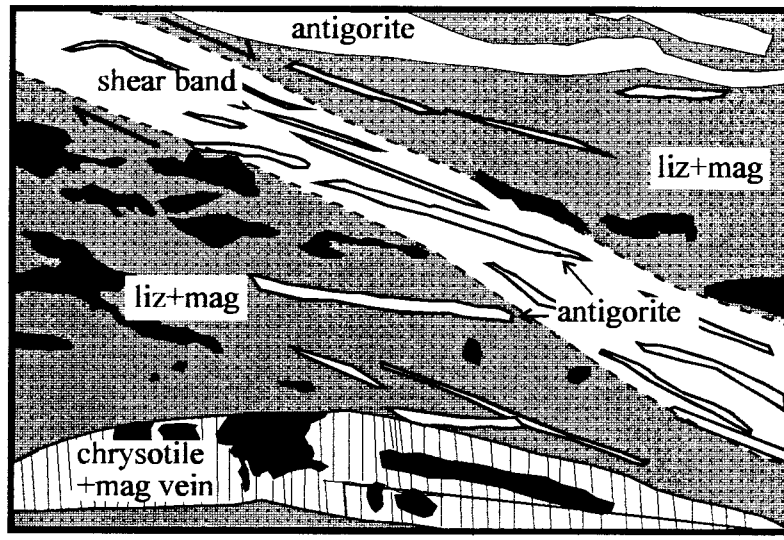

Figure 5-6 Antigorite shear band cross-cutting lizardite band, with late chrysotile vein, Toll Road shear zone (Coulton and others, unpublished data). Field of view 1.5mm.

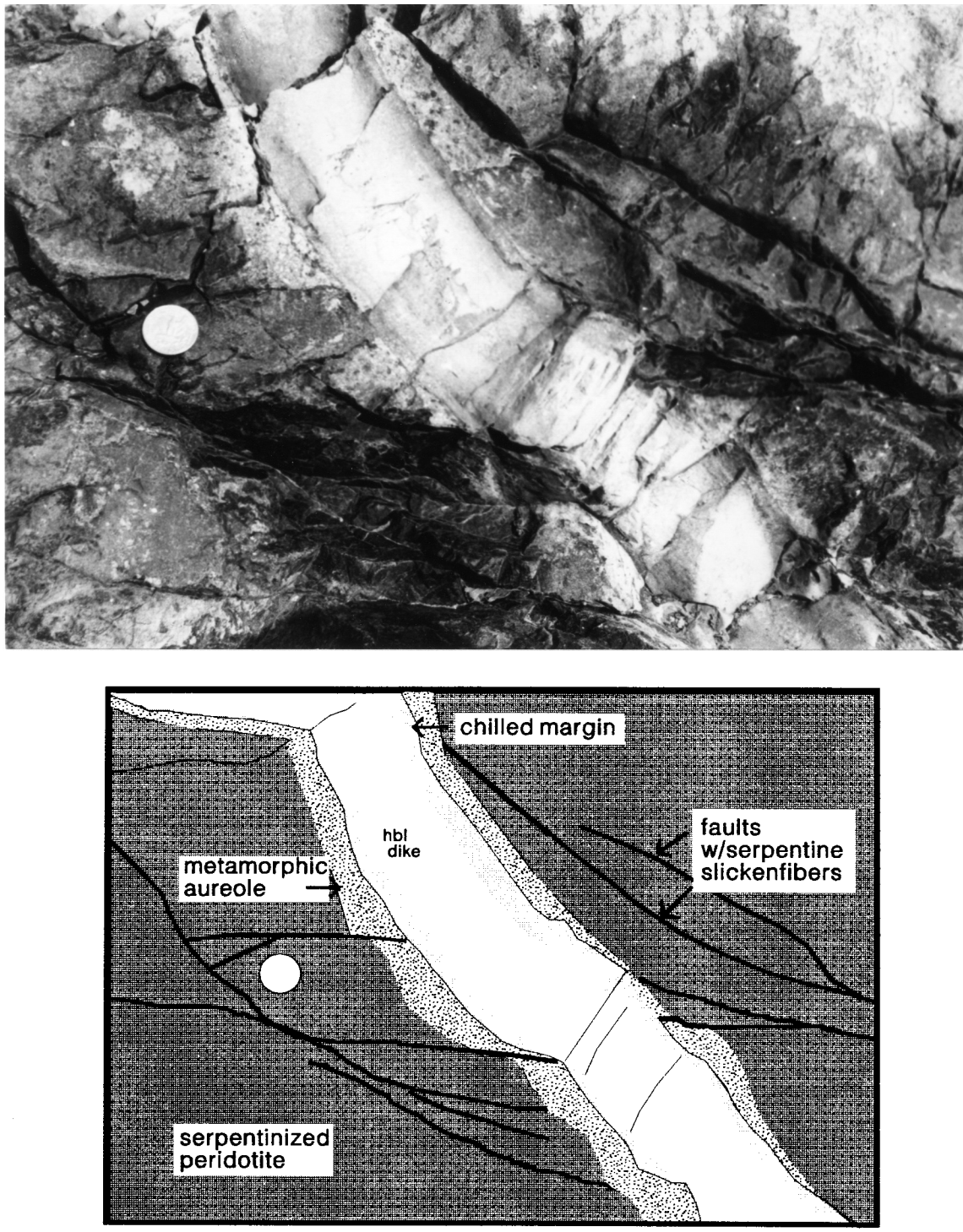

Figure 6-7 Outcrop photograph and sketch of water-polished outcrop in Josephine Creek showing diabase dike cross-cutting fault-bounded serpentinite blocks in brittle fault zone. Dike is chilled against serpentinite and narrow contact metamorphic aureole overprints pre-existing serpentine.

Figure 6-9 Relict lizardite and magnetite partially overprinted by needles of antigorite within antigorite mylonite from basal sole. Field of view 2 mm

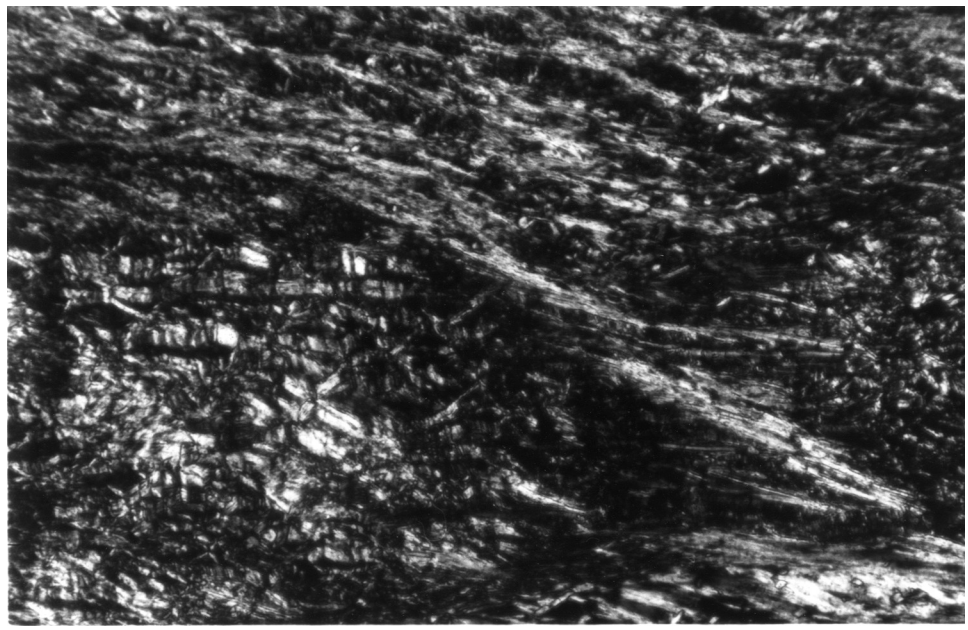

Figure 6-10 Photomicrograph of serpentinite mylonite in TRSZ. Relict lizardite partially overprinted by shear bands of antigorite (see color photograph, chapter 4). Field of view 1mm

A

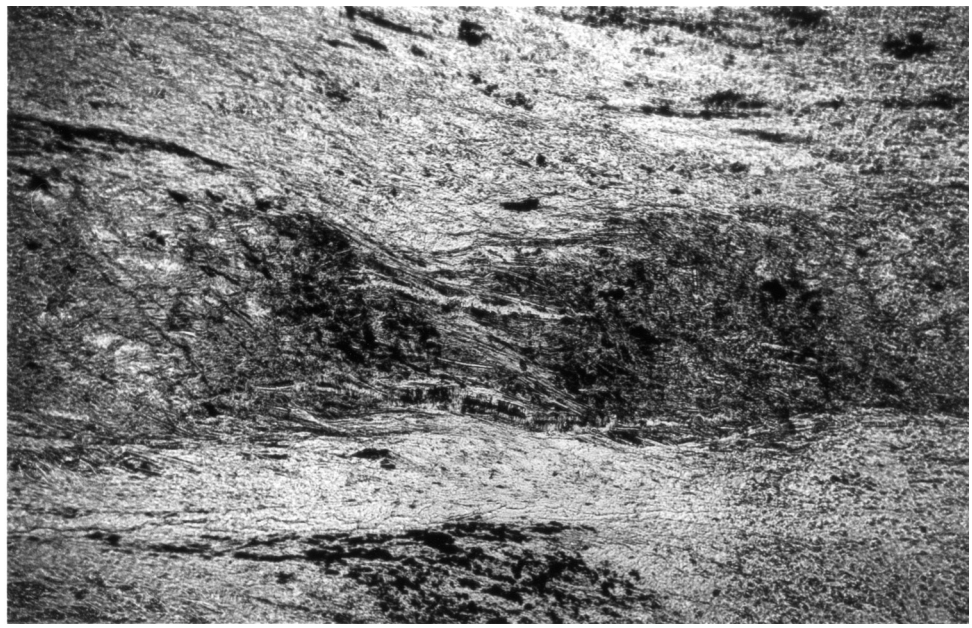

Figure7- 5 Microphotographs of serpentinites showing critical textural relationships between antigorite, lizardite and chrysotile and/or deformation (A) antigorite shear band cross-cutting 1 mm wide lizardite band within antigorite mylonite, TRSZ, PPL, scale bar 1 mm (B) Subparallel lizardite and magnetite bands, lizardite partially replaced by antigorite blades, Basal sole, XPL, scale bar 1 mm (C) Antigorite + dolomite extension vein cross-cutting deformed antigorite + lizardite serpentinite, PCSZ, XPL, vein 0.5 mm wide.

B

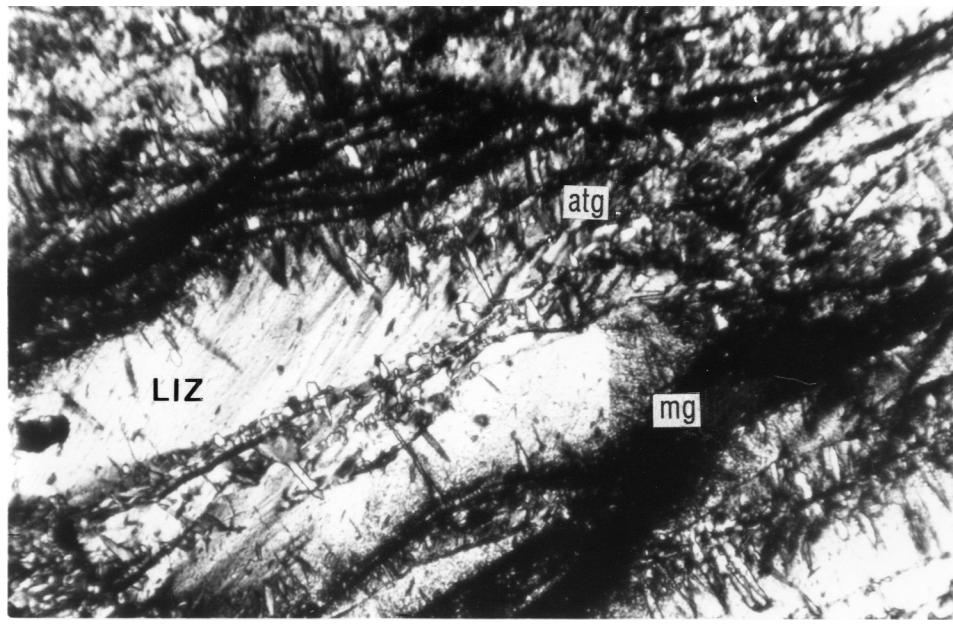

C

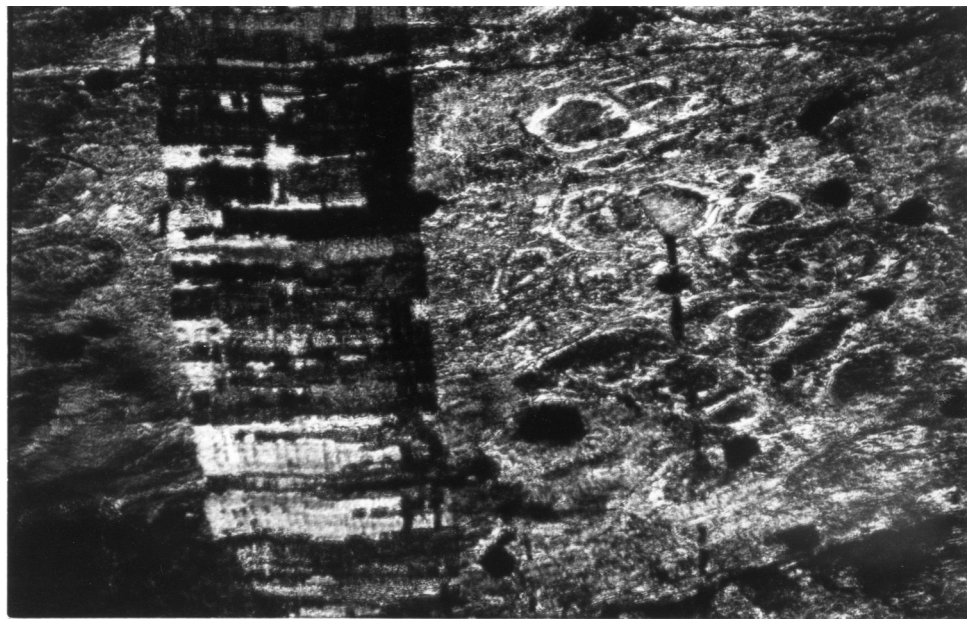

MICROBEAM X-RAY DIFFRACTION

X-ray diffraction patterns produced by microbeam x-ray diffraction are shown on the following page.

Serpentine minerals were identified using diagrammatic templates drawn from Wicks and Zussman (1975), Figure 5. Representive diagrammatic diffraction patterns are shown in Figure 3.1.

Sample numbers followed by (1), (2), A or B indicate samples of different textures within the same thin-section.

Left to right from top row:

PCM 1A	antigorite
PCM 4	lizardite 1T
PCM 5A (1)	lizardite 1T
PCM 5A (2)	antigorite + minor lizardite
PCM 9	antigorite
PC 26A	antigorite
PC 26B	lizardite 1T

Note: All samples identified by microbeam x-ray diffraction are from the Patrick Creek shear zone. Microbeam x-ray diffraction was used to identify the mineralogy of characteristic serpentine textures, and to aid the choice of samples for stable isotope analysis. Powder samples analysed for oxygen and hydrogen isotopic composition were analysed separately by the powder x-ray diffraction method (see following section)

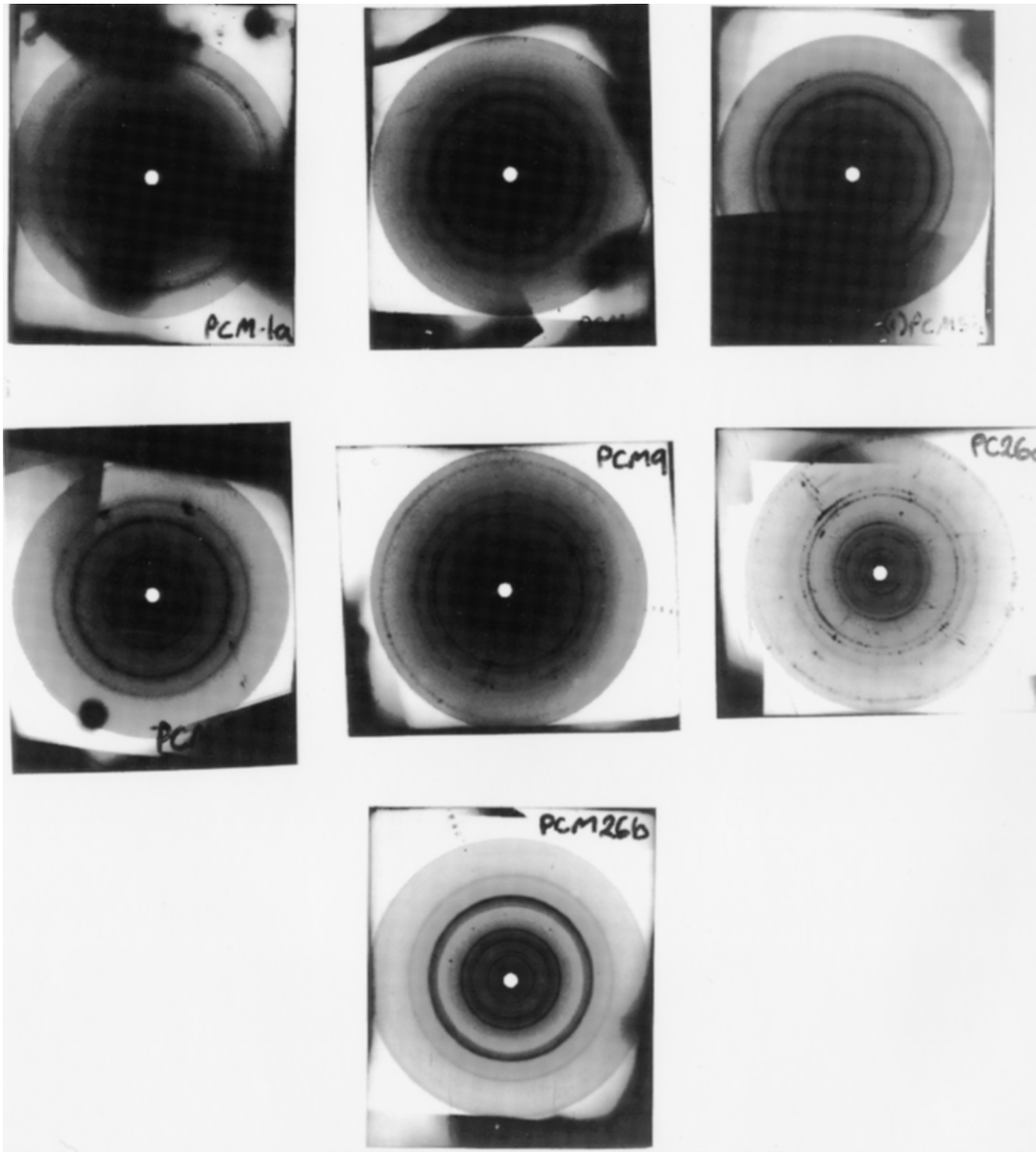
PCM-1a
PCM9
PC26a
PCM26b